

Structural Damage Detection via a Combination of Pso and Bayesian Reliability Analysis

*Ling Yu²⁾ and Zepeng Chen¹⁾

¹⁾ *Department of Mechanics and Civil Engineering, Jinan University, Guangzhou 510632, China*

^{1), 2)} *MOE Key Lab of Disaster Forecast and Control in Engineering, Jinan University, Guangzhou 510632, China*

²⁾ *lyu1997@163.com*

ABSTRACT

Different kind of methodologies have been presented in the last decades and achieved broad applications in structural damage detection (SDD). Particle swarm optimization (PSO) based algorithms have been confirmed to be effective for SDD. The method avoids inversion computation which is prone to be ill-posed or ill-conditioning. However, the accuracy of optimization algorithm is affected by its randomness although it is the theoretical basis of algorithm. Repeated calculations are often performed to gain an average value of SDD results, but the computing cost increases simultaneously. In this study, a novel two-step SDD method is proposed via a combination of PSO and Bayesian reliability analysis. It consists of two major steps, i.e., SDD and Bayesian reliability analysis. Firstly, SDD on structures is achieved by the PSO – improved Nelder-Mead method (PSO-INM). a new objective function, so-called multi-sample objective function, is proposed based on Bayesian theory. The Bayesian reliability analysis is then performed for a further analysis, the most likely damaged elements are distinguished from the spurious ones. Finally, some numerical simulations on SDD of a 2-storey rigid frame are used to assess the effectiveness of the proposed method, some related issues are discussed as well.

1. INTRODUCTION

Structural damage detection (SDD) techniques are methodologies that use structural static or dynamic responses to assess the structural operating condition. The stiffness of structures is one of the most common used index to diagnose the extent of damages. In the last two decades, SDD have been popularly investigated and achieved greatly successes in the field of structural health monitoring (SHM). The basic idea of SDD is to find the changed structural properties from measured responses before and after severe events such as hurricane, earthquake, deterioration due to aging and so on (Farrar and Worden 2007; Li and Chen 2013). For a better description of structural damage, a class of models are generally defined based on an assumed relationship

²⁾ Professor

between input and output variables of the structural system (Teughels and De Roeck 2005). Such model-based techniques transfer the SDD process into minimizing the difference between the measured and theoretical output data of the structures, which named model updating. The output data for model updating is divided into two major parts, time domain data and frequency domain data (Yu and Lin 2015). Time domain data such as accelerations are rarely used directly for modal updating as it requires precise knowledge of the input excitation (Simoen et al. 2015). On the contrary, frequency domain data, which are extracted from the measured responses, are independent of the input excitation. The advantages make frequency domain data more popular in model updating. Frequency domain data such as frequency, mode shape, modal flexibility (Pandey and Biswas 1994), modal curvature (Pandey et al. 1991), and modal strain energy (Shi et al. 2000) have been widely used and employed for structural model updating.

Generally, an objective function (or cost function, fitness function) is needed to be pre-established for model updating based on the measured and theoretical output data, and SDD is achieved by minimizing the objective function. In other words, model updating problem is equivalent to a constrained optimization problem. SDD is a typical inverse problem (Friswell 2008) and traditional methodologies using decomposition methods, such as singular value decomposition (SVD), QR factorization or Cholesky factorization, and regularization techniques to solve the problem involved ill-posedness inevitably (Simoen et al. 2015). The ill-posedness result in a very unstable solution with respect to small changes in the measured data.

To overcome this difficulty, some computational techniques, such as genetic algorithm (GA) (Yan et al. 2007), ant colony optimization (ACO) (Yu and Xu 2011), artificial fish swarm algorithm (AFSA) (Pandey and Biswas 1994), firefly algorithm (FA) (Pan et al. 2016) and PSO (Baghmisheh et al. 2012; Seyedpoor 2012) have been proposed for solving SDD problems. Among these techniques, the PSO based algorithm has been confirmed effective due to its good performance in global searching. PSO is simple in concept and didn't involve inverse analysis. However, the accuracy of the optimization algorithm is affected by its randomness which is the theoretical basis of the algorithm. The randomness of PSO, such as particle initial distribution and random numbers containing in the manipulating equation, ensures the algorithm to search the whole feasible space but sometimes makes it fall into the wrong solution, which are generally called local optimum. However, the PSO algorithm has been improved to deal with such weakness. Baghmisheh et al. (2012) adopted a hybrid PSO-NM algorithm for damage assessment based on PSO and Nelder–Mead simplex algorithm (NM). Seyedpoor et al. (2012) proposed a two-step algorithm which reduce the dimension of optimal parameters leading a more accurate results.

Another factor affects the accuracy of PSO is the uncertainty of model and response data. Due to the complex and indeterminate environment around the structure, the output data tends to show significant variation from one test to the next. The disturbance of environments are described as noise. Therefore, idealized numerical prediction models are unable to perfectly represent behaviors of the structure. Probabilistic analysis is a common used method for uncertainty quantification (Simoen et al. 2015). Probability density functions (PDFs) are always pointed to the uncertain variables and hypothesis test is applied to assess the reliability of structural damages

identified by PSO-INM. Bayesian method is a well-known theorem among probabilistic analysis methods. Beck (Beck et al. 1999; Cheung and Beck 2009; Ching and Beck 2004) and Yuen (Yuen et al. 2004; Yuen and Kuok 2011) have made great efforts to establish the Bayesian statistical framework for SHM. Beck firstly presented a Bayesian statistical framework for system identification and applied the theory to continual on-line SHM using vibration data from structures.

Actually, the random searching ability of the PSO and the noise contaminated in the output data both lead to an unstable solution. To address the deficiency, the probabilistic analysis would be a good way to assess the solution and improve its accuracy. In this paper, a novel two-step SDD method is proposed. In the first step, an objective function based on Bayesian theory, named multi-sample objective function, is proposed to reduce the influence of noises and the objective function is optimized by the PSO-INM algorithm. In the second step, a post posterior probability analysis is presented based on Bayesian methodology to distinguish real damage elements from possible ones. Numerical simulations on a 2-storey rigid frame using frequencies and mode shapes information show the proposed method is effective for accurately identifying the location and extent of multiple structural damages.

2. Theoretical background

2.1 SDD formulation

SDD problem has been deeply investigated in the field of SHM. Based on model-base methods, the damage is considered as reduction of stiffness and mass of structures. Assuming the change in mass can be ignored comparing with the stiffness (Begambre and Laier 2009). Then, the linear relationship between structural stiffness matrix and element stiffness matrix can be adopted as follows:

$$\mathbf{K}(\boldsymbol{\theta}) = \sum_{i=1}^{N_e} (1 - \theta_i) \mathbf{K}_i \quad (1)$$

in which $\boldsymbol{\theta}$ is a vector of damage factor with same length of N_e element numbers and ranges from 0 to 1. $\theta_i = 0$ means the undamaged condition. \mathbf{K} and \mathbf{K}_i represent structural global stiffness matrix and i -th element stiffness matrix respectively. The dynamic behavior of structural finite element model (FEM) under excitation force $\mathbf{F}(t)$ can be written as:

$$\mathbf{M}\ddot{\mathbf{u}} + \mathbf{C}(\boldsymbol{\theta})\dot{\mathbf{u}} + \mathbf{K}(\boldsymbol{\theta})\mathbf{u} = \mathbf{F}(t) \quad (2)$$

where \mathbf{M} , $\mathbf{C}(\boldsymbol{\theta})$ are structural mass and damping matrix, respectively. $\ddot{\mathbf{u}}$, $\dot{\mathbf{u}}$, \mathbf{u} are corresponding to acceleration, velocity and displacement vector respectively. The m -th undamped frequency ω_m and mode shape $\boldsymbol{\phi}_m$ are extracted from the characteristic equation derived from Eq. (2):

$$\left[\mathbf{M} - \omega_m^2 \mathbf{K}(\boldsymbol{\theta}) \right] \boldsymbol{\phi}_m = \mathbf{0} \quad (3)$$

2.2 PSO-INM algorithm

The PSO-INM is a method for solving the model updating problem described above. It is hybrid algorithm combining PSO and improved Nelder-Mead method (INM). The

basic idea of *PSO-INM* is to search the local area around optimum solution θ^* found by PSO using INM. The INM's perfect local searching ability helps to increase the θ^* 's precision. Some more details of PSO-INM algorithm is referred in Chen and Yu (2015).

Traditional objective function is usually based on modal data, i.e., the relative percentage errors (RPE) of frequencies and the modal assurance criterion (MAC) of the mode shapes in the following form,

$$\theta^* = \arg \min_{\theta} F(\theta) = \arg \min_{\theta} \left[\sum_{m=1}^{N_m} 1 - MAC(\varphi_m^c, \varphi_m^a) + RPE(\omega_m^c, \omega_m^a) \right] \quad (4)$$

where $MAC(\varphi_m^c, \varphi_m^a) = \frac{|\varphi_m^{cT} \varphi_m^a|^2}{|\varphi_m^{cT} \varphi_m^c| |\varphi_m^{aT} \varphi_m^a|}$, ($m = 1, 2, \dots, N_m$) represents MAC of calculated m -th mode shape φ_m^c and actual m -th mode shape φ_m^a within the first N_m modal data.

$RPE(\omega_m^c, \omega_m^a) = \left| \frac{\omega_m^a - \omega_m^c}{\omega_m^a} \right| \times 100\%$, ($m = 1, 2, \dots, N_m$) is the RPE between the calculated m -th frequency ω_m^c and the actual frequency ω_m^a . When the calculated modal data equal to the actual ones, the objective function gets its minimum value of zero. The corresponding solution θ^* is regarded as the structural condition.

For real structures, actual data are contaminated noise. The noise in the numerical simulation is considered as a zero-mean stationary Gaussian white-noise added up to original frequency domain data in different damage cases. The formulation of this process can be described as follows:

$$\mathbf{D}_{noise} = \mathbf{D} + \varepsilon \psi \mathbf{R} \quad (5)$$

where \mathbf{D}_{noise} , \mathbf{D} are the measured data for noise and noiseless, respectively. ε is the noise level ranging from 0 to 1 and \mathbf{R} is a vector with random values obeying the distribution $N(0, 1)$. ψ is the value of frequency for frequency data and is calculated by Eq. (6) where mode shapes have N_n nodes.

$$\psi = \sqrt{\frac{1}{N_n N_m} \sum_{n=1}^{N_n} \sum_{m=1}^{N_m} \varphi_{nm}^2} \quad (6)$$

2.3 Bayesian theory

To remove the noise negative effect from the optimal process, the idea of Bayesian theory is referred to form a more effective objective function and help to distinguish spurious damaged elements out of the solution.

The probabilistic SHM framework based on Bayesian theory was firstly presented by Beck (Beck et al. 1999) and applied for an simulating on-line monitoring. The significant basic of Bayesian theory is the conditional probability, which assumed the prior knowledge attributed to a certain events or hypothesis. The Bayesian interpretation provide a rigorous process for uncertainty quantification. Bayesian theory used in the field of SHM to express the updated probabilities of model parameter θ has the mathematical form as:

$$p(\theta|\mathbf{D}) = cp(\mathbf{D}|\theta)p(\theta) \quad (7)$$

where $p(\boldsymbol{\theta}|\mathbf{D})$ is the probability density function (PDF) of model parameters given the modal data \mathbf{D} and the assumed FEM, and $p(\mathbf{D}|\boldsymbol{\theta})$ is the PDF of modal data given the model parameter, which is more widely known as likelihood function. $p(\boldsymbol{\theta})$ is the prior PDF of model parameters $\boldsymbol{\theta}$ based on engineering and modeling judgments. c is a constant which ensures the integral of $p(\boldsymbol{\theta}|\mathbf{D})$ to be one. Taking $\mathbf{D}=\{\mathbf{D}_1, \mathbf{D}_2, \dots, \mathbf{D}_{N_s}\}$ as the observing modal data with N_s samples. And $\mathbf{D}_s=\{\omega_{1,s}, \omega_{2,s}, \dots, \omega_{N_m,s}, \boldsymbol{\varphi}_{1,s}, \boldsymbol{\varphi}_{2,s}, \dots, \boldsymbol{\varphi}_{N_m,s}\}$ represents s -th sample of frequencies and mode shapes. Then the likelihood function becomes:

$$p(\mathbf{D}|\boldsymbol{\theta})=\prod_{s=1}^{N_s} p(\mathbf{D}_s|\boldsymbol{\theta})=\prod_{s=1}^{N_s} \left(\prod_{m=1}^{N_m} p(\omega_{m,s}|\boldsymbol{\theta}) p(\boldsymbol{\varphi}_{m,s}|\boldsymbol{\theta}) \right) \quad (8)$$

It is assumed that the testing and modal data are independent. The principle of maximum entropy is used as a justification to choose a Gaussian distribution for the $\omega_{m,s}$ and $\boldsymbol{\varphi}_{m,s}$ distribution. Then the resulting PDFs of $\omega_{m,s}$ and $\boldsymbol{\varphi}_{m,s}$ are

$$p(\omega_{m,s}|\boldsymbol{\theta})=c_1 \exp \left[-\frac{(\omega_{m,s}-\omega_m^a)^2}{2\varepsilon_m^2} \right] \quad (9)$$

$$p(\boldsymbol{\varphi}_{m,s}|\boldsymbol{\theta})=c_2 \exp \left[-\frac{1}{2\delta_m^2} (\boldsymbol{\varphi}_{m,s}-\boldsymbol{\varphi}_m^a)^T (\boldsymbol{\varphi}_{m,s}-\boldsymbol{\varphi}_m^a) \right] \quad (10)$$

where, ε_m^2 and δ_m^2 are the variance of the m -th frequency and the diagonal element of covariance matrix C_m , respectively. The covariance matrix C_m of m -th mode shape is simplified as $C_m=\delta_m^2 I_{N_n \times N_n}$. The sample variances are used to approximate the variances of Gaussian distribution ε_m^2 and δ_m^2 which can be calculated as follows:

$$\varepsilon_m^2=\frac{1}{N_s-1} \sum_{s=1}^{N_s} (\omega_{m,s}-\omega_m^a)^2, \quad \delta_m^2=\frac{1}{N_s-1} \sum_{s=1}^{N_s} \|\boldsymbol{\varphi}_{m,s}-\boldsymbol{\varphi}_m^a\|^2 \quad (11)$$

The initial PDF on model parameters $\boldsymbol{\theta}$ is assumed to have the form:

$$p(\boldsymbol{\theta})=c_3 \exp \left[-\frac{1}{2\sigma^2} (\boldsymbol{\theta}-\boldsymbol{\theta}_0)^T (\boldsymbol{\theta}-\boldsymbol{\theta}_0) \right]=c_3 \exp \left(-\frac{1}{2\sigma^2} \boldsymbol{\theta}^T \boldsymbol{\theta} \right) \quad (12)$$

The choice of $\boldsymbol{\theta}_0$ is $[0, 0, \dots, 0]^T$ which represents the undamaged case. The individual parameters are assumed to be independent, i.e., the covariance matrix of $\boldsymbol{\theta}$ is a diagonal one. Here, the choice for σ^2 reflect the level of uncertainty in structures.

Substituting Eqs. (9), (10) and (12) into Eq. (8) yields the final form of $p(\boldsymbol{\theta}|\mathbf{D})$:

$$p(\boldsymbol{\theta}|\mathbf{D})=c \exp \left[-\sum_{s=1}^{N_s} \sum_{m=1}^{N_m} \left[\frac{(\omega_{m,s}-\omega_m^a)^2}{2\varepsilon_m^2} + \frac{(\boldsymbol{\varphi}_{m,s}-\boldsymbol{\varphi}_m^a)^T (\boldsymbol{\varphi}_{m,s}-\boldsymbol{\varphi}_m^a)}{2\delta_m^2} \right] -\frac{1}{2\sigma^2} \boldsymbol{\theta}^T \boldsymbol{\theta} \right] \quad (13)$$

The goal of Bayesian-based probabilistic analysis is to maximize the probability of $p(\boldsymbol{\theta}|\mathbf{D})$ based on the known testing data and then ascertain the most likely damaged

elements.

$$\boldsymbol{\theta}^* = \arg \min_{\boldsymbol{\theta}} F(\boldsymbol{\theta}) = \arg \min_{\boldsymbol{\theta}} \left\{ \sum_{s=1}^{N_s} \sum_{m=1}^{N_m} \left[\frac{(\omega_{m,s} - \omega_m^a)^2}{2\varepsilon_m^2} + \frac{(\boldsymbol{\varphi}_{m,s} - \boldsymbol{\varphi}_m^a)^T (\boldsymbol{\varphi}_{m,s} - \boldsymbol{\varphi}_m^a)}{2\delta_m^2} \right] \right\} \quad (14)$$

Based on the Bayesian analysis process, a multi-sample objective function is proposed related to Eq. (13), which can be written as Eq. (14). The aim of the multi-sample objective function is to make full use of the data sets but not only use the average value. The advantages of multi-sample objective function will be explored in the next section.

After defining the multi-sample objective function, the PSO-INM is conducted to search the minimum value of Eq. (14). Generally, the PSO-INM will run several times to avoid randomness, the average value is selected as the final solution. Error will increase if some extremely high local solution is involved. So, a post posterior probability of identified solutions is presented based on Bayesian analysis process. The analytical process is similar to the above description except replacing the modal data with the identified solutions calculating by the PSO-INM. It is rational to deem the randomness of PSO-INM as another kind of uncertainty. Then the randomness of PSO-INM and noise contaminated data can be considered together as system uncertainty. Assuming $\mathbf{D} = \{\boldsymbol{\theta}_1, \boldsymbol{\theta}_2, \dots, \boldsymbol{\theta}_{N_t}\}$ is the identified solutions found by the PSO-INM during N_t run times, based on Eq. (13), the PDF of $p(\boldsymbol{\theta}|\mathbf{D})$ given the data \mathbf{D} is as follows,

$$p(\boldsymbol{\theta}|\mathbf{D}) = c \exp \left[-\sum_{t=1}^{N_t} \frac{(\boldsymbol{\theta}_t - \boldsymbol{\theta})^T (\boldsymbol{\theta}_t - \boldsymbol{\theta})}{2\delta^2} - \frac{1}{2\sigma^2} \boldsymbol{\theta}^T \boldsymbol{\theta} \right] \quad (15)$$

3. Numerical Simulations

3.1 Two-story rigid frame structure

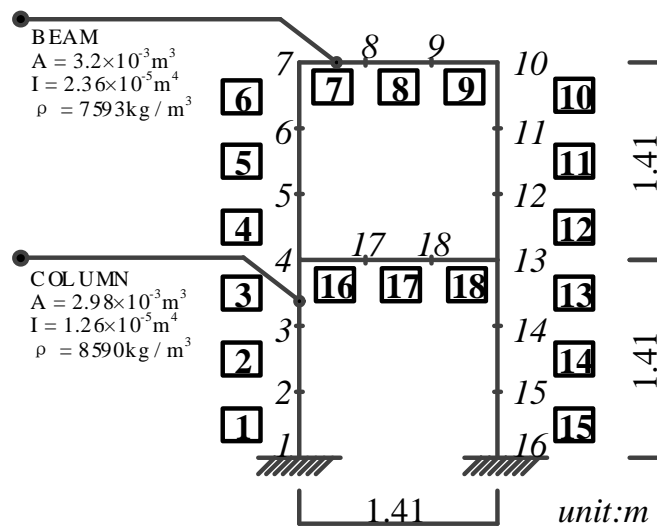


Fig. 1 Finite element model of two-story rigid frame structure

A two-story rigid frame structure is adopted to assess the performance of the proposed method. The diagram of structure, physical dimensions and material properties are as shown in Fig. 1. The elastic modulus of both beam and column are equal to $2.1 \times 10^{11} \text{ N/m}^2$. The numbers in the box represent the finite element number, while others denote the measured node number.

The frame structure is modeled by eighteen two-dimension beam elements with equal length. Several damage scenarios are simulated by setting different value in the damage coefficient vector θ . Single damage is introduced in the 17th element ranging from 5% to 40%. Different combination of elements with different damage extents are simulated to identify the multi-damage cases. The damage element location and extent are listed in Table 1. The symbol 5%@17 in Table 1 indicates that the stiffness of the 17th element is decreased by 5%, similar meaning for other cases.

Table 1 Damage cases

Cases	Description
1	5%@17
2	10%@17
3	20%@17
4	40%@17
5	20%@8, 20%@17
6	10%@8, 20%@17
7	15%@5, 20%@8, 30%@17
8	25%@5, 25%@8, 25%@11, 25%@17

The first five modal frequencies and mode shapes are adopted, which means $N_m = 5$. The mode shape is measured along the vertical direction of components, which means that the vertical direction of beam and the horizontal direction of column are available. Noise is contaminated in the frequency and mode shape based on Eq. (5). Frequencies are contaminated 3% noise while the mode shapes are contaminated 5%, respectively.

3.2 Comparison on different objective functions

Case 3 is used to investigate effects of noise on objective functions. Assuming the damage location is determinate, the objective function becomes a single variable function with respect to damage extent at 17th element. Noises are added up to the original modal data in Case 3 to generate 100 samples. Dividing these data into 10 groups with equal sample size of 10. The objective functions, based on Eqs. (4) and (14) respectively, are calculated using different group of data. The average values of each group data are adopted for traditional objective functions. Fig. 2(a) is the result due to traditional objective function while Fig. 2(b) is for the proposed one. The left plot of each figure describes the trend of objective function value with respect to damage extent at 17th element and the right one demonstrates the optimal damage extent corresponding to the minimal objective function value for every group. By comparison, the optimal damage extent of multi-sample objective function in Fig. 2(b), which varied within a small area, is more stable than the traditional one in Fig. 2(a). Under the effect of noise, the optimal solution of traditional objective function deviated from the actual

one and would lead to error identification even if the algorithm has a great optimal ability. On the contrary, the optimal solution of multi-sample objective function is stable for different group of data. This advantages of multi-sample objective function make it more suitable for optimal algorithm and help to improve the accuracy of results.

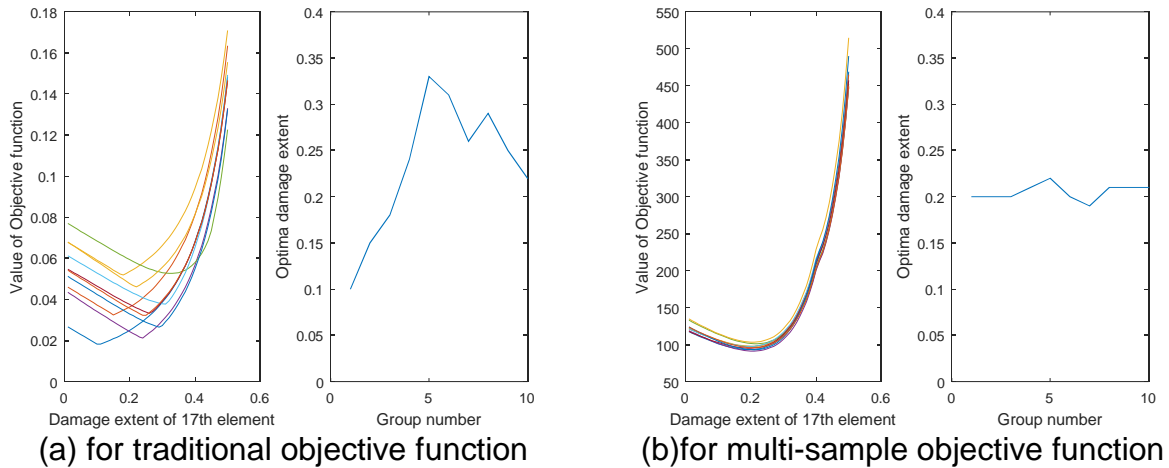


Fig. 2 Comparison on results due to objective functions

3.2 Sample size for objective functions

Because the multiple samples are available in the proposed objective function, the sample size is an important parameter to be assessed. A small sample size cannot guarantee the stability of objective functions while the large one would waste the computing resource. The sample size is assessed by single damage cases for convenience. The optimal damage extent in Cases 2 to 4 with respect to sample size are shown in Fig. 3. It can be found from Fig. 3 that the optimal damage extents become gradually stable with increasing sample size. When the sample size is higher than 10, the optimal damage extents of all the single cases remain around the real one. Therefore, the sample size is set to be 10 and extended for other multi-damage cases.

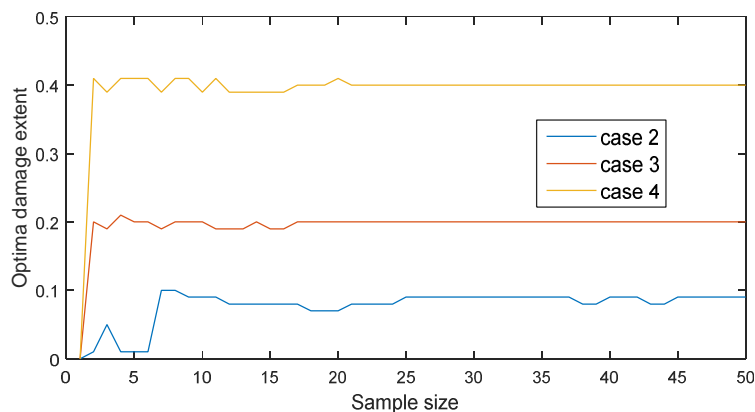


Fig. 3 Optimal damage extent with respect to sample size

3.3 Damage identification results

As shown in Table 1, there are 4 single damage cases with damage at 17th element.

All the calculation results using the PSO-INM are shown in Fig. 4. And 50 runs are conducted for each scenario. The sample size is 10 and the average values are adopted for traditional objective function. The symbol “Bayesian case 1” and “Traditional case 1” in Fig. 4(a) mean the results for Case 1 using multi-sample objective function and traditional objective function respectively, similar meaning for other cases.

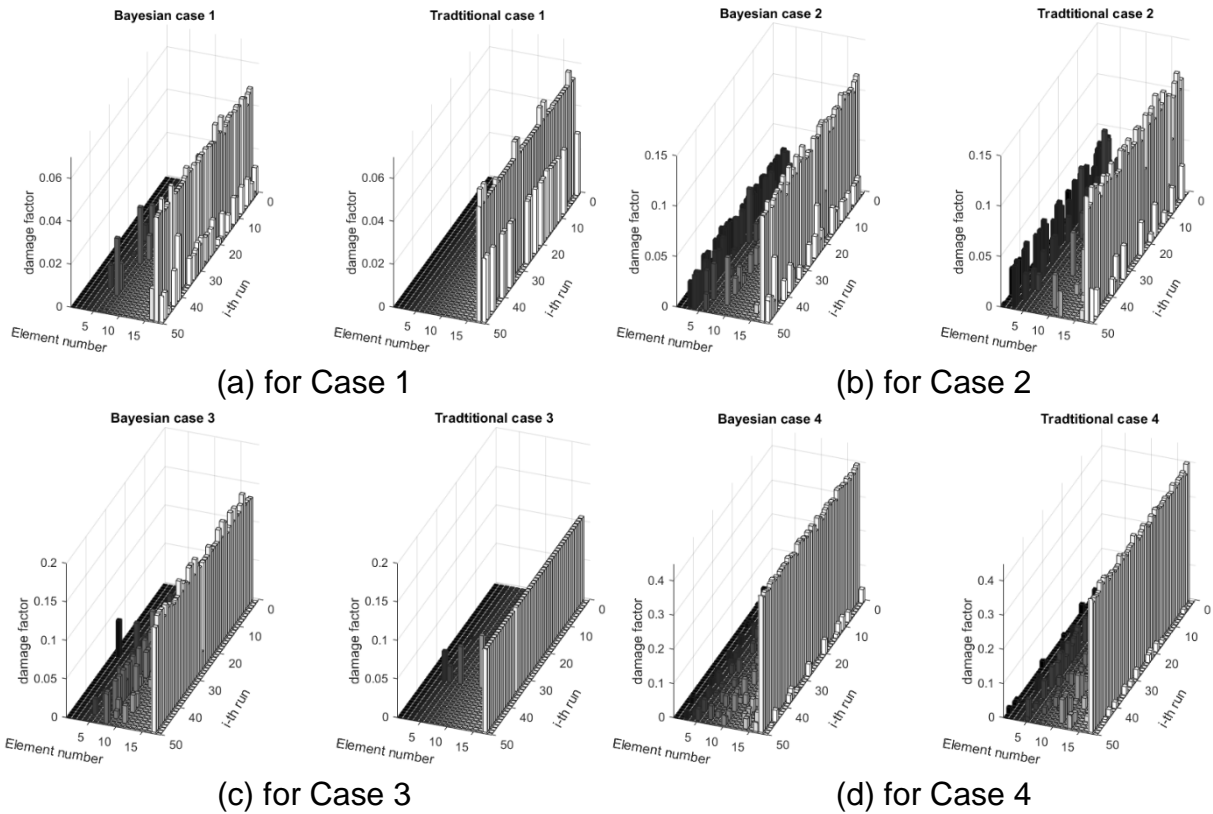


Fig. 4 Damage identification for all single cases

Fig. 4 shows that the damage factor at 17th element is obviously greater than that at other elements. It means that the damage location can be assessed well. Some error identified elements also exist mostly around the 17th element, such as 16th and 18th elements. The identified result for Case 2 is the worst one where elements around the 3rd element keep a quite high value of damage factor. The identified damage at 18th element in Case 1, as shown in Fig. 4(a), is smaller than that in Bayesian case, which means that the multi-sample objective function outperform than the traditional one in the case of small damage, i.e. 5% stiffness reduced in element. After the damage gradually increases, both objective functions show their advantage in assessing the damage location and extent because effects of stiffness change in modal data predominate the noise.

The identified results for multi-damage scenarios, i.e., Cases 5 to 8 as listed in Table 1, are shown in Fig. 5. For the multi-damage scenarios, the multi-sample objective function shows its greater capability of assessing damage than the traditional one. The conclusion can be confirmed strongly from Case 6, which includes two damages

occurring in 8th and 17th elements respectively. As shown in the left histogram of Fig. 6(b), the bars at 8th and 17th elements are higher than others with more stable values. Therefore, the damage locations are assessed in the two elements and the corresponding damage extent can be adopted by their average values. On the contrary, there are at least four stable bars in the right histogram of Fig. 6(b), which means two health elements are misjudged as damaged elements using traditional objective function. However, the results for Case 8 in Fig. 5(d) further prove that the multi-sample objective function is more accurate in quantifying the damage extent than that due to the traditional objective function. Case 8 has four damaged elements with equal stiffness reduction. The left histogram in Fig. 5(d) shows this state clearly, while the right one shows that the damage factors at 5th and 11th elements are obviously lower than that at 8th and 17th elements.

The illustrated results for both single and multiple damage scenarios indicate that the multi-sample objective function not only locate the structural damage effectively but also quantify the damage extent with an improved higher accuracy.

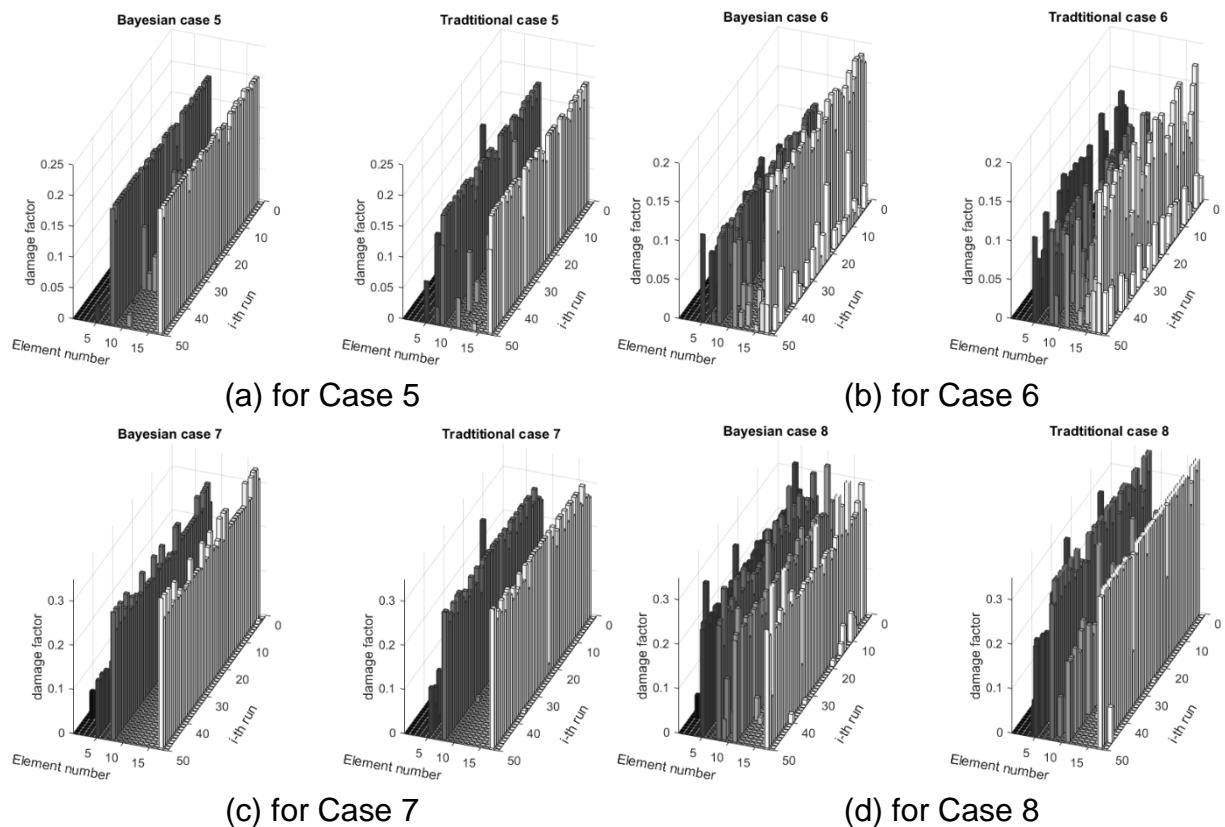
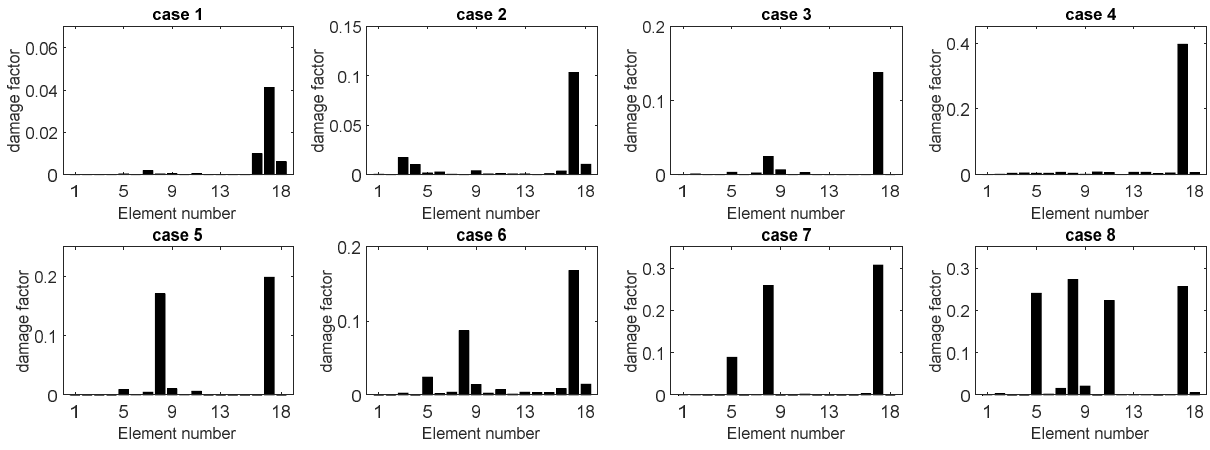


Fig. 5 Damage identification for multi-damage cases

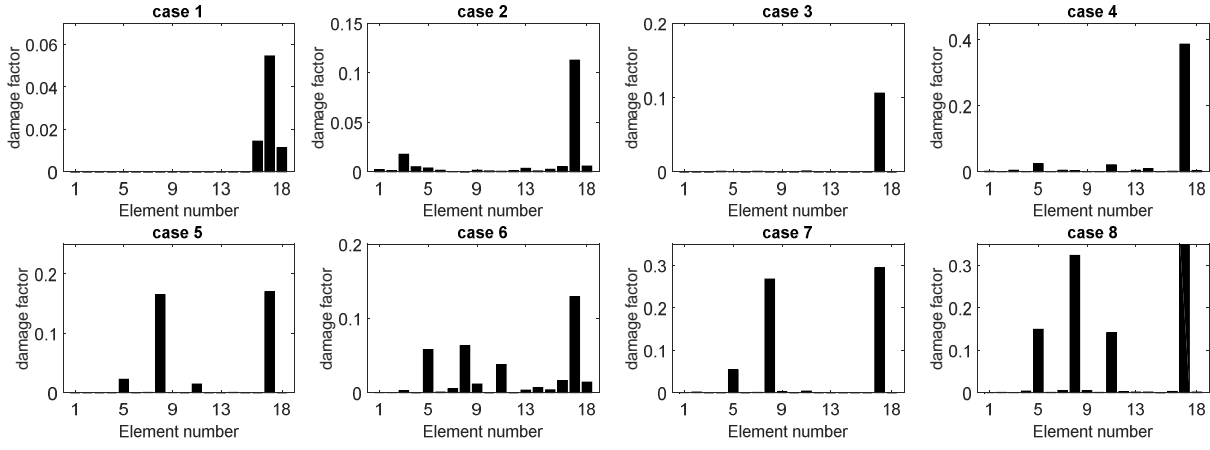
3.4 Probabilistic analysis based on Bayesian theory

Usually, the average value of results calculated by the PSO-based algorithm are used to represent the final solution. Fig. 6(a) shows the average solution due to multi-sample objective function while Fig. 6(b) is due to traditional objective function. Base on the average value, same conclusions can be drawn that the multi-sample objective function outperform the traditional objective function in both locating multi-damage and

quantifying damage extent. However, some undamaged elements with a non-negligible damage, such as 16th and 18th elements in Case 1, 3rd element in Case 2, and 5th element in Case 6, lead to puzzlement in judging actual damage elements. It is better to find a way to filter these spurious damage elements and improve the identification accuracy further.



(a) Average value due to multi-sample objective function



(b) Average value due to tradition objective function

Fig. 6 Average value of damage identified results

Based on the Bayesian theory as described in section 2.3, Eq. (15) is adopted to analyze the identified solutions found by the PSO-INM. First of all, a prior PDF of model parameters θ based on engineering and modeling judgments should be determined. Assuming the covariance matrix of initial model parameters is a diagonal matrix with same value $\sigma^2=0.05\|\Delta\theta\|^2$, where $\Delta\theta$ represents the maximum absolute error of the estimated parameters and 0.05 reflects the level of uncertainty. The damage extent lower than 0.001 is deemed as health element in this paper. The possible damage elements, with a damage extent higher than 0.001, are upgraded based on Eq. (15). The PSO-INM is used again for this upgrading process. Fig. 7 shows the post probabilistic analysis of the possible damage elements. The black bar represents the

mean value due to the multi-sample objective function while the white one means the average value of further analysis based on probabilistic analysis. The Bayesian theory based analysis leads to a decreasing damage extent among possible damage elements, but the decrease in spurious damage elements are greater than the actual damage elements which make the actual damage elements more outstanding.

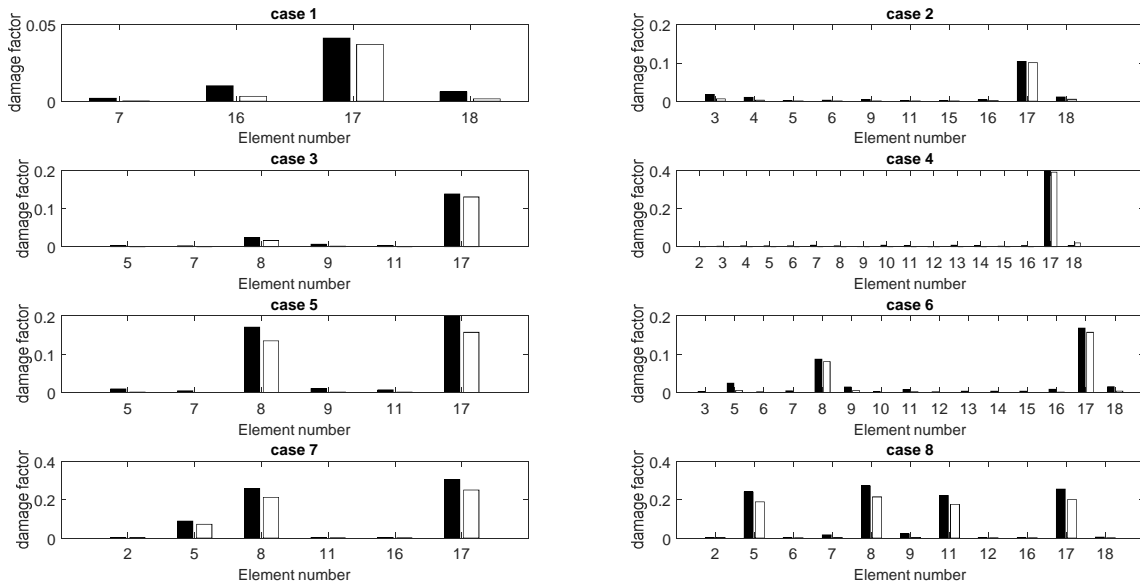


Fig. 7 Comparison on average value of damage results

4. CONCLUSIONS

Based on the Bayesian theory, a multi-sample objective function is proposed for SDD issues. Comparative studies between the proposed objective function and the traditional one are conducted in this paper. To distinguish the spurious damage elements from the actual ones, the Bayesian probabilistic analysis is introduced after the process of PSO-INM. Numerical simulations on a two-story rigid frame shows that the method proposed in this paper can not only locate the structural damages effectively but also quantify the damage extent with an improved higher accuracy. Some conclusions can be summarized as follows:

1. The multi-sample objective function based on Bayesian theory avoid excessively bias of minimum point of objective function. It helps to improve the accuracy of PSO-based algorithm because the optimum of multi-sample objective function is closer to the actual damage cases. The disadvantage of noise is greatly reduced.
2. The multi-sample objective function outperform in identified small damages and multiple damages. The ability is more suitable for actual structures, where damages should be detected before extending and more than one damage exist simultaneously.
3. By introducing Bayesian-based probabilistic analysis after the PSO-based algorithm, the spurious damage elements can be rejected and the actual damage becomes more outstanding.

ACKNOWLEDGEMENTS

The project is jointly supported by the National Natural Science Foundation of China with grant numbers 51278226 and 50978123 respectively.

REFERENCES

- Baghmisheh, M.T.V., Peimani, M., Sadeghi, M.H., Etefagh, M.M., and Tabrizi, A.F. (2012). "A hybrid particle swarm–Nelder–Mead optimization method for crack detection in cantilever beams." *Appl. Soft. Comput.*, **12**(8): 2217-2226.
- Beck, J.L., Au, S.K., and Vanik, M.W. (1999). "Bayesian probabilistic approach to structural health monitoring." *J. Eng. Mech.*, **126**(7): 738-745.
- Begambre, O., and Laier, J.E. (2009). "A hybrid particle swarm optimization – simplex algorithm (PSOS) for structural damage identification." *Adv. Eng. Softw.*, **40**(9): 883-891.
- Chen, Z.P., and Yu, L. (2015). "An improved PSO-NM algorithm for structural damage detection" International Conference on Swarm Intelligence, Beijing, China
- Cheung, S.H., and Beck, J.L. (2009). "Bayesian model updating using hybrid monte carlo simulation with application to structural dynamic models with many uncertain parameters." *J. Eng. Mech.*, **135**(4): 243-255.
- Ching, J., and Beck, J.L. (2004). "Bayesian analysis of the phase II IASC-ASCE structural health monitoring experimental benchmark data." *J. Eng. Mech.*, **130**(10): págs. 1233-1244.
- Farrar, C.R., and Worden, K. (2007). "An introduction to structural health monitoring." *Philos. Trans. R. Soc. A*, **365**(1851): 1-17.
- Friswell, M.I. (2008). "Damage identification using inverse methods." *Philos. Trans. R. Soc. A*, **365**(1851): 393-410.
- Li, Y.Y., and Chen, Y. (2013). "A review on recent development of vibration-based structural robust damage detection." *Struct. Eng. Mech.*, **45**(2): 159-168.
- Pan, C.D., Yu, L., Chen, Z.P., Luo, W.F., and Liu, H.L. (2016). "A hybrid self-adaptive Firefly-Nelder-Mead algorithm for structural damage detection." *Smart. Struct. Syst.*, **17**(6): 957-980.
- Pandey, A.K., and Biswas, M. (1994). "Damage detection in structures using changes in flexibility." *J. Sound Vib.*, **169**(1): 3-17.
- Pandey, A.K., Biswas, M., and Samman, M.M. (1991). "Damage detection from changes in curvature mode shapes." *J. Sound Vib.*, **145**(2): 321-332.
- Seyedpoor, S.M. (2012). "A two stage method for structural damage detection using a modal strain energy based index and particle swarm optimization." *Int. J. Nonlin. Mech.*, **47**(1): 1-8.
- Shi, Z.Y., Law, S.S., and Zhang, L.M. (2000). "Structural damage detection from modal strain energy change." *J. Eng. Mech.*, **126**(12): 1216-1223.
- Simoen, E., De Roeck, G., and Lombaert, G. (2015). "Dealing with uncertainty in model updating for damage assessment: A review." *Mech. Syst. Signal Pr.*, **56–57**: 123-149.
- Teughels, A., and De Roeck, G. (2005). "Damage detection and parameter identification by finite element model updating." *Arch. Comput. Method E.*, **12**(2): 123-164.
- Yan, Y.J., Cheng, L., Wu, Z.Y., and Yam, L.H. (2007). "Development in vibration-based structural damage detection technique." *Mech. Syst. Signal Pr.*, **21**(5): 2198-2211.
- Yu, L., and Lin, J.C. (2015). "Cloud computing-based time series analysis for structural damage detection." *J. Eng. Mech.*, doi: 10.1061/(ASCE)EM.1943-7889.0000982 , C4015002.
- Yu, L., and Xu, P. (2011). "Structural health monitoring based on continuous ACO method." *Microelectron Reliab.*, **51**(2): 270-278.
- Yuen, K.-V., Au, S.K., and Beck, J.L. (2004). "Two-stage structural health monitoring approach for phase I Benchmark studies." *J. Eng. Mech.*, **130**(1): 16-33.
- Yuen, K.V., and Kuok, S.C. (2011). "Bayesian methods for updating dynamic models." *Appl. Mech. Rev.*, **64**(1): 3-7.